Structural Transformations of sVI *tert*-Butylamine Hydrates to sII Binary Hydrates with Methane

Pinnelli S. R. Prasad,[†,‡] Takeshi Sugahara,[†,§] E. Dendy Sloan,[†] Amadeu K. Sum,[†] and Carolyn A. Koh*[,†]

Center for Hydrate Research, Chemical Engineering Department, Colorado School of Mines, Golden, Colorado 80401, Gas Hydrates Division, National Geophysical Research Institute, Council for Scientific and Industrial Research, Hyderabad 500606, India, and Division of Chemical Engineering, Graduate School of Engineering Science, Osaka University, Toyonaka, Osaka 560-8531, Japan

Received: July 9, 2009; Revised Manuscript Received: September 2, 2009

Binary clathrate hydrates with methane (CH_4, 4.36 Å) and *tert*-butylamine (*t*-$BuNH_2$, 6.72 Å) as guest molecules were synthesized at different molar concentrations of *t*-$BuNH_2$ (1.00−9.31 mol %) with methane at 7.0 MPa and 250 K, and were characterized by powder X-ray diffraction (PXRD) and Raman microscopy. A structural transformation from sVI to sII of *t*-$BuNH_2$ hydrate was clearly observed on pressurizing with methane. The PXRD showed sII signatures and the remnant sVI signatures were insignificant, implying the metastable nature of sVI binary hydrates. Raman spectroscopic data on these binary hydrates suggest that the methane molecules occupy the small cages and vacant large cages. The methane storage capacity in this system was nearly doubled to ∼6.86 wt % for 5.56 mol % > *t*-$BuNH_2$ > 1.0 mol %.

Introduction

Gas hydrates (clathrate hydrates) are nonstoichiometric inclusion compounds in which gaseous guest molecules are trapped in a host lattice formed by water molecules in an ice-like hydrogen-bonded framework. Gas hydrates exist as a stable solid phase in permafrost regions and in ocean-floor sediments around the world.[1] Substantial amounts of natural gas (mostly methane) are trapped in condensed form in hydrates (typically 1 m^3 of hydrate has 164 m^3 of STP equivalent methane). In hydrate applications of energy recovery, transportation, and storage, it would be highly desirable to alter the gas hydrate stability conditions to manageable limits by using inhibitors/promoters.[2]

Three common gas hydrate structures are currently known: sI (structure I), sII (structure II), and sH (structure H); sI and sII are the most predominant structures for all natural gas hydrates. Structure I can host molecules such as methane, ethane, and carbon dioxide, while structure II can host larger molecules such as propane and isobutane, or very small molecules, such as hydrogen. Structure H requires a coguest molecule, such as methylcyclohexane, in addition to methane and is an attractive storage system for higher amounts of fuel gas.[3]

The crystal structure of gas hydrates consists of a number of polyhedra (cages), which are primarily comprised of pentagonal and hexagonal faces. For example, the small cages of both sI and sII consist of 12 pentagons (5^{12}).[2] The large cages in sI and sII each have additional hexagonal faces; the sI large cage has 12 pentagonal and two hexagonal faces ($5^{12}6^2$), while the large cage of sII has 12 pentagonal and four hexagonal faces ($5^{12}6^4$). The unit cell of sI contains two 5^{12} and six $5^{12}6^2$ cages, and the sII unit cell has sixteen 5^{12} and eight $5^{12}6^4$ cages.[2] On the other hand, sH consists of three types of cages: the large cage ($5^{12}6^8$) is occupied by a large guest molecule, and the other two cages, 5^{12} and $4^35^66^3$, are occupied by small molecules such as methane. Additionally, several other clathrate structures denoted sIII to structure VII (sVII) were proposed by Jeffery,[4,5] and structure-T (sT) was proposed by Udachin et al.[6] These structures, with the exception of structures IV and V, have been experimentally verified.[2]

In particular, structure VI hydrate with *tert*-butylamine is attractive because it is the only possible clathrate structure with an estimated hydrogen storage capacity approaching the U.S. DOE target of 5.5 wt % by 2015, assuming full occupancy of the small cages and fractional occupancy (>0.8) of the large cages with hydrogen in sVI.[7] The *t*-$BuNH_2$ clathrate hydrate is known to crystallize into a cubic sVI hydrate, which consists of two types of cages: 8-hedra (4^45^4) and 17-hedra ($4^35^96^27^3$). The diameters for the small and large cages are 5.8 and 10.2 Å, respectively. In sVI hydrate, *t*-$BuNH_2$ molecules occupy the large cages, leaving the small cages vacant.[4,5] Recently, Kim et al.[8] have reported a structural transformation in sVI *t*-$BuNH_2$ hydrates [16 *t*-$BuNH_2 \cdot 156\ H_2O$] to sII upon pressurizing an aqueous solution of *t*-$BuNH_2$ with methane at 70 bar and 283.65 K. From size constraints for small guests in the sVI cages, it appears impossible to fill the small cages (4^45^4) of sVI with methane (guest to cage size ratio is 1.453).[9] Furthermore, we have also shown that sVI *t*-$BuNH_2$ hydrates undergo structural transformation in the presence of hydrogen.[9] These observations have triggered concern on the stability of sVI hydrates in the presence of coguest molecules capable of occupying the small cages. Kim et al.[8,10] reported that the NMR spectral signature of binary hydrates (CH_4 + *t*-$BuNH_2$) has mixed structures of (sVI + sII) with *t*-$BuNH_2$ molar concentrations of 9.3 and 7.0 mol %; pure sII with *t*-$BuNH_2$ molar concentrations of 5.6 and 4.5 mol %; (sI + sII) with *t*-$BuNH_2$ molar concentrations of less than 3.0 mol %; and sI in binary hydrates with *t*-$BuNH_2$ < 0.5 mol %. To gain insight into the structural stability of sVI hydrate, particularly in the range 9.31 mol % > *t*-$BuNH_2$ > 5.56 mol %, we investigated the binary hydrate formation with methane gas using *tert*-butylamine clathrate (sVI) as the starting

* Corresponding author. Tel.: (303) 273-3237. Fax: (303) 273-3730. E-mail: ckoh@mines.edu.
† Colorado School of Mines.
‡ National Geophysical Research Institute.
§ Osaka University.

10.1021/jp906492j CCC: $40.75
Published on Web 09/28/2009

material rather than an aqueous *t*-$BuNH_2$ + CH_4 gas mixture. These experimental conditions we believe would not only prevent simultaneous growth of sVI and sII, but also probe the solid-state transformation process. The binary hydrates were characterized by powder X-ray diffraction (PXRD) and Raman microscopy, and the stored methane gas was measured by volumetric gas release measurements.

Experimental Method

The *t*-$BuNH_2$ clathrate hydrate samples were synthesized from specific amounts (0.98−9.31 mol %) of *t*-$BuNH_2$ (Sigma-Aldrich) and deionized water at 258 K and ambient pressure. The solution was vigorously stirred until hydrates formed, at which point the hydrates were stored in a freezer at ∼250 K for about 10−15 h. The hydrate (finely ground powder) was added to a pressure vessel, which was precooled to below 200 K. During preliminary experiments, we used a lower CH_4 pressure (5.0−5.5 MPa) and realized that the signatures of sII were not prominent and a considerable amount of ice signatures were also observed, as measured by the PXRD (see Figures S1−S3 in the Supporting Information). Therefore, we conducted all subsequent experiments at higher CH_4 pressures (7.0 MPa), which were also consistent with earlier experiments,[8] while maintaining the temperature at 250 K for formation of the binary (*t*-$BuNH_2$ + CH_4) hydrate in the solid state. The cell was maintained at these conditions over a period of 48 h (at a constant temperature of 250 K) for the enclathration of CH_4 into the hydrate. The cell was immersed in liquid nitrogen for about 15−20 min and then degassed. The binary hydrate was analyzed by powder X-ray diffraction (PXRD) and Raman spectroscopy.

The PXRD measurements were performed on a Siemens D500 diffractometer with Co radiation (wavelength 1.788965 Å) in the $\theta/2\theta$ scan mode. The measurements were performed in the step scan mode with a dwell time of 2 s and step size of 0.02°. The PXRD pattern was collected in the range 2θ = 8−65°; measurements were carried out at ambient pressure and 100 K. The PXRD pattern indexing and cell refinement were obtained using the Checkcell and PowderX programs.[11] Raman spectroscopic measurements were performed using a LabRam HR spectrometer (JY Instruments) with a 532 nm excitation source providing 6 mW at the sample. All of the measurements were recorded at ambient pressure and near liquid nitrogen temperature.

For the volumetric gas release measurements, the binary hydrates were prepared using a procedure similar to that described above. Residual gas in the cell was decreased to atmospheric pressure at around ∼200 K. The cell was connected to a gasometer (Ruska Inc.) to measure the amount of gas released. The maximum uncertainty originating from the measurement of the initial hydrate mass (±0.05 g) and released methane gas volume (±5.0 mL) upon decomposition was around 5%. These measurements were made with samples of about 3−5 g of presynthesized *t*-$BuNH_2$ hydrates; the binary hydrates were completely dissociated to obtain the amount of gas released. We have not estimated the accurate binary hydrate mass as the PXRD results show small quantities of residual *t*-$BuNH_2$ in the hydrate samples. For convenience, we expressed the released methane as mL/g, which refers to the gas released (mL) per gram sample (which consists of pure *t*-$BuNH_2$ hydrate and residual ice).

Results and Discussion

Figure 1 shows the PXRD patterns of pure *t*-$BuNH_2$ and *t*-$BuNH_2$ + CH_4 hydrates. As seen in Figure 1a, it is clear that

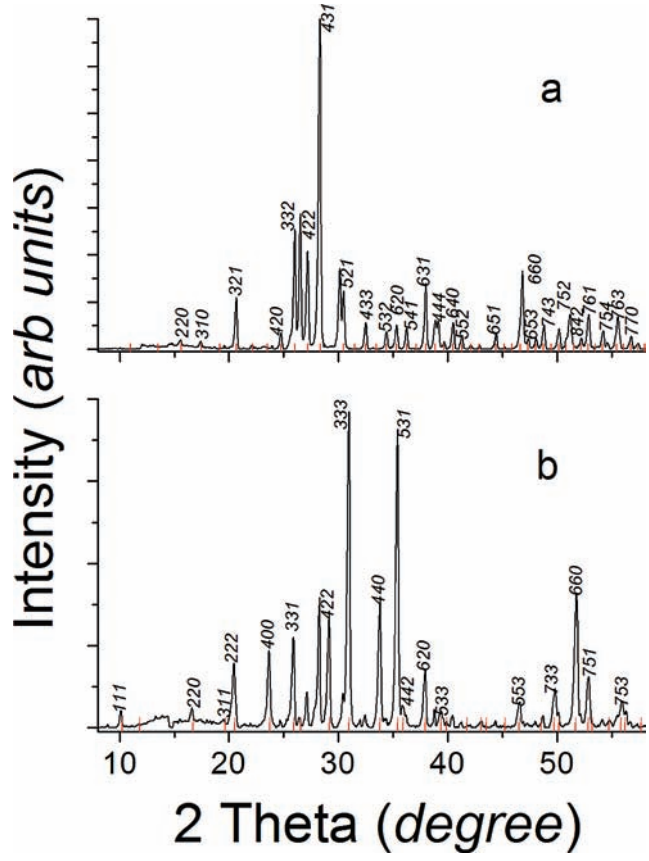

Figure 1. Powder X-ray diffraction patterns of pure *t*-$BuNH_2$ (a) and binary (*t*-$BuNH_2$ + CH_4) hydrates with *t*-$BuNH_2$ 7.3 mol % (b) recorded at ambient pressure and 100 K. The pure *t*-$BuNH_2$ clathrate hydrate was pressurized with methane (7.0 MPa and 250 K). Vertical bars at the bottom of each graph represent the generated 2θ values using the optimized unit cell parameters (see text).

the starting material, synthesized with 7.3 mol % of *t*-$BuNH_2$, can be indexed to a mixture of sVI and ice, indicating that the *t*-$BuNH_2$ hydrates crystallized into a cubic *I3d* structure even when the mole fraction is less than the stoichiometric composition of 9.31 mol %. An earlier reported parameter (a = 18.81 Å[4,8]) was used as an initial estimate to obtain the refined unit cell parameter of a = 18.6341 ± 0.0046 Å. The red vertical bars along the abscissa in Figure 1 indicate the generated 2θ values. It is interesting to notice that the pure sVI *t*-$BuNH_2$ hydrate decomposes at 272 K.[4,12] The eutectic point for the *t*-$BuNH_2$ + H_2O binary system has been reported at −8 °C (265 K) and ∼4 mol % *t*-$BuNH_2$.[12] A similar procedure was used to analyze the PXRD data for the binary *t*-$BuNH_2$ + CH_4 clathrate hydrates. The resulting PXRD pattern for *t*-$BuNH_2$ (7.3 mol %) + CH_4 hydrates (Figure 1b) was better fitted to a sII hydrate (space group *Fd3m*) with a lattice constant of a = 17.3984 ± 0.0177 Å. We also observed a similar PXRD pattern for *t*-$BuNH_2$ (5.86 mol %) + CH_4 hydrates, which was also indexed to sII with a = 17.4898 ± 0.0225 Å. Negligible amounts of unconverted sVI were identified in the patterns for the binary *t*-$BuNH_2$ + CH_4 hydrates.

From the PXRD results, it is evident that a structural transformation from sVI to sII occurred when hydrate samples initially with only *t*-$BuNH_2$ were pressurized with CH_4. Kim et al.[8,10] reported the coexistence of sVI and sII for *t*-$BuNH_2$ concentrations between 7.0 and 9.31 mol % in the binary (*t*-$BuNH_2$ + CH_4) hydrate system, whereas sII was the preferred structure at lower concentrations (5.6−4.5 mol %) of the large guest molecule. It is worth noting that the preparation procedure

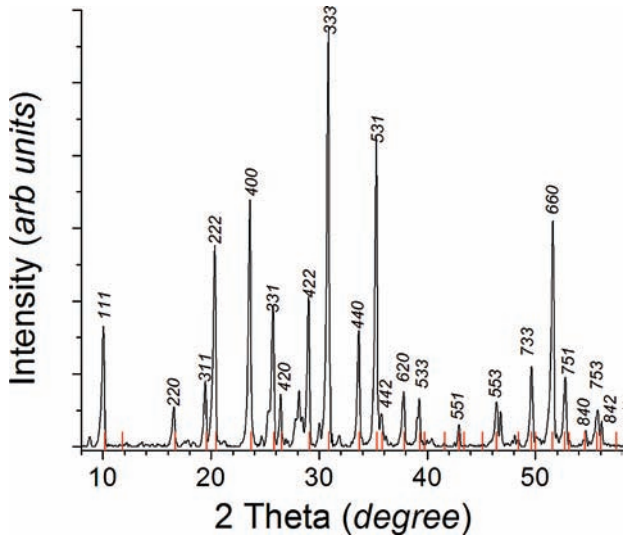

Figure 2. Powder X-ray diffraction pattern for t-$BuNH_2$ (8.81 mol %) + H_2 binary clathrates recorded at ambient pressure and 100 K. The binary hydrates were prepared by pressurizing solid t-$BuNH_2$ and ice powder.

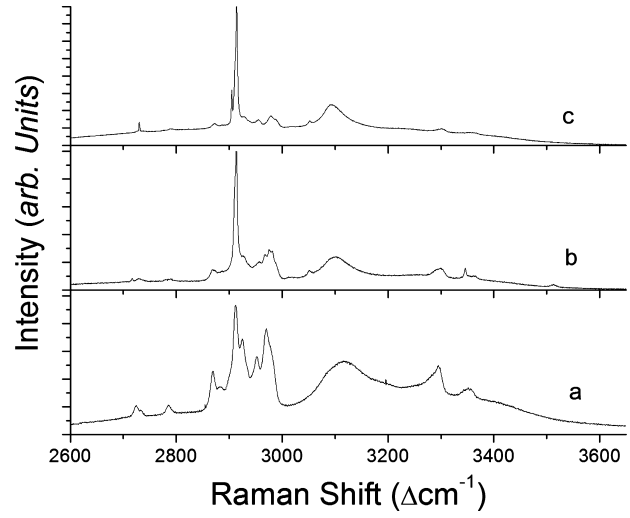

Figure 3. Raman spectra of t-$BuNH_2$ clathrates (a) and binary t-$BuNH_2$ + CH_4 hydrates in the 2600−3650 cm^{-1} region with t-$BuNH_2$ 9.31 mol % (b) and 8.29 mol % (c). The spectra were recorded at 100 K and atmospheric pressure.

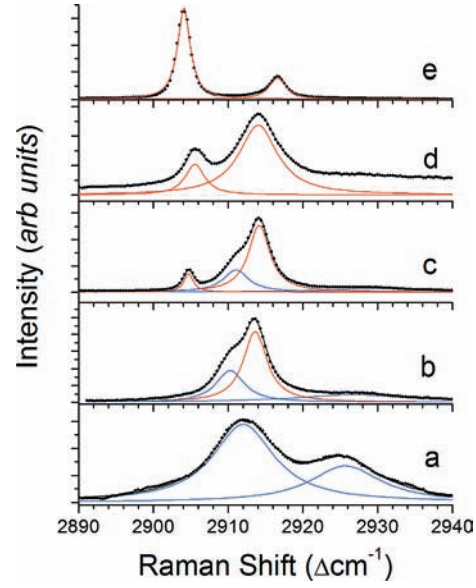

Figure 4. The Raman spectra of enclathrated methane (red) and t-$BuNH_2$ (blue) molecules in the characteristic CH stretching mode region. The concentration of t-$BuNH_2$ is 9.31% (a), 9.31% (b), 8.29% (c), 3.0% (d), and 1.0% (e). The spectral traces (b)−(e) are with CH_4 as coguest in binary t-$BuNH_2$ + CH_4 hydrates, while (a) is without CH_4.

by Kim et al.[8,10] was different; they used 70 bar (7.0 MPa) of methane pressure and aqueous solution with t-$BuNH_2$ and decreased the temperature from 293.15 to 270.15 K to form hydrates, whereas our studies aimed at probing the transformation using presynthesized solid t-$BuNH_2$ hydrate. By considering the size of the guest molecules and the available cage sizes, it is suggested that the t-$BuNH_2$ molecules can occupy the large cages of both sVI (size ratio of 0.908) and sII (size ratio of 1.009). On the other hand, the methane molecules are too large to be stored in the small cages of sVI (size ratio of 1.453), thus triggering the structural transformation, irrespective of the t-$BuNH_2$ concentration. Our PXRD results are consistent with this reasoning, and sII signatures are observed for binary hydrates with (t-$BuNH_2$ + CH_4).

To further confirm the formation of the sII double hydrates, we performed experiments using the mixture (8.81 mol %) of ice and solid t-$BuNH_2$ as a starting material. Upon pressurizing the solid mixture in the presence of small cage guest molecules, the PXRD pattern was sII, and most of the recorded lines could be indexed to space group $Fd3m$ with lattice constant of a = 17.4535 ± 0.0132 Å (Figure 2). Here, we used hydrogen gas rather than methane because of the smaller molecular size of hydrogen, which was capable of occupying the small cages (4^45^4) of sVI. The remnant phase signatures for sVI in the PXRD pattern were negligibly small. From these experiments, it is concluded that the sVI phase is metastable for binary hydrates.

Further evidence for enclathration of CH_4 in binary hydrates in t-$BuNH_2$ + CH_4 was obtained from Raman spectroscopy. The characteristic Raman modes for CH_4 enclathrated in 5^{12} cages at 2915 cm^{-1} have a strong overlap with t-$BuNH_2$ bands. To distinguish the bands between different guest molecules, CH_4 and t-$BuNH_2$, we compared the Raman spectrum of pure t-$BuNH_2$ clathrate and binary clathrates with different molar concentrations of t-$BuNH_2$ as shown in Figures 3 and 4. In Figure 3, the Raman spectrum in the range 2800−3400 cm^{-1} is convoluted with many bands due to CH_3 and NH_2 groups of *tert*-butylamine. In particular, the asymmetric and symmetric stretching modes for the NH_2 group are at 3352 and 3294 cm^{-1}. Earlier studies[13] of the H_2O + t-$BuNH_2$ system have shown that the Raman intensities and band positions strongly depend on the molar concentration of t-$BuNH_2$, and the present study matches well with the reported Raman band at 3294 cm^{-1} for t-$BuNH_2$ < 20 mol %. On the other hand, the stronger symmetric stretching bands for CH_3 groups have two components at 2913 and 2926 cm^{-1} (see Figure 4) in the vicinity of the characteristic methane modes for the clathrate hydrates. The corresponding mode in H_2O + t-$BuNH_2$ was earlier reported at 2920 cm^{-1}, and it was also shown that the Raman intensity and position for this mode are independent of molar concentration.[13] Additionally, the Raman spectrum in the range 2800−3000 cm^{-1} consisting of other modes of CH_3 has features similar to those reported earlier.[13] The (OH) stretching mode observed at 3115 cm^{-1} in t-$BuNH_2$ clathrate and the binary hydrate is also comparable to that reported in the literature.[14−17]

When pressurized with methane, a new band around 2915 cm^{-1} is clearly observed along with other CH_3 groups of t-$BuNH_2$ (Figure 4). The Raman shift and line width for these

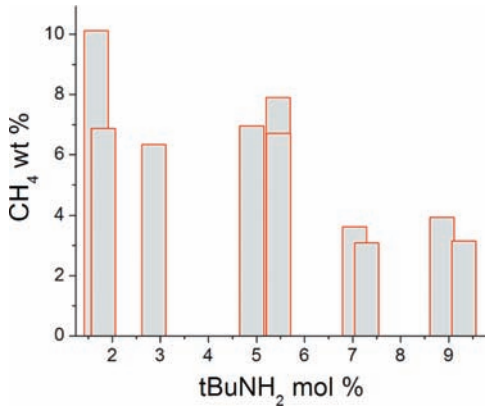

Figure 5. Histograms showing the amount of methane released during the dissociation of binary hydrates with t-$BuNH_2$ + CH_4. Overlapping bars correspond to repeat experiments.

modes could not be attributed to the free methane gas, but instead are due to methane trapped in 5^{12} cages of sI or sII. However, from the PXRD (Figure 1), it is evident that the structure of the binary clathrate is sII, and thus the Raman mode is assigned to methane trapped in 5^{12} cages of sII. The binary hydrates with lower concentration of t-$BuNH_2$ show some interesting features in the Raman spectrum. A new mode around 2905 cm^{-1} in the binary hydrates with t-$BuNH_2$ (8.29 mol %) is clearly observed (Figure 4 c), a signal that remained observable in successive dilutions of t-$BuNH_2$. This mode corresponds to methane molecules encaged in $5^{12}6^4$ cages of sII.[2,15,16] However, in binary hydrates with THF or t-$BuNH_2$, it is generally assumed that the large cages are only occupied by the larger guest molecules. Contrary to this knowledge, recent studies have shown that the methane molecules could be also entrapped in vacant large cages of sII.[15,18,19] Molecular dynamics simulations were recently employed to study the methane storage potential of various hydrate forming structures (sI, sII, and sH).[20] These studies have shown that decreasing the sII hydrate formers such as propane or THF to 1−3 mol % increases the methane storage capacity; however, higher methane pressures are essential during hydrate formation.[20] The important features of hydrates with two guest molecules such as methane and THF, for the "tuning effect" to achieve better storage of fuel gas, were summarized by Seo et al.[21] All of the hydrate forming systems (sI, sII, and sH) studied so far on the tuning and structural transformations effects have the 5^{12} cages as the common cage; however, sVI with pure t-$BuNH_2$ is an exception. Furthermore, the Raman spectrum (Figure 4e) of binary hydrates with t-$BuNH_2$ (<1.0 mol %) is dominated by the sI hydrate structure, corroborating earlier NMR studies,[8,10] which report sI structure for binary hydrates with t-$BuNH_2$ concentrations < 2.0 mol %.

It is interesting to notice that the absolute methane gas stored in the binary hydrates significantly increases when the concentration of t-$BuNH_2$ is close to the sII stoichiometry (Figure 5). The results show that the storage capacity of methane in the hydrate is low (3.45 wt %) at higher t-$BuNH_2$ concentrations (7.0 < t-$BuNH_2$ mol % < 9.31). Gas released from these samples was 64 mL CH_4/g, at ∼0.083 MPa pressure and 297 K. Note that from the PXRD results, almost all hydrate crystals were determined to be sII. The released methane gas is much lower than that expected for sII hydrates with t-$BuNH_2$ molecules in the large cages and CH_4 in the small cages ($\theta_s^{sII} \approx 0.6986$), indicating there are a significant number of vacant small cages. Additional amounts of t-$BuNH_2$ (>5.56 mol %) may be significantly influencing the methane occupancy of the 5^{12} cages. Furthermore, Kim et al.[10] have also noticed that the t-$BuNH_2$ molecules having the tendency to form sVI inhibit the formation of both sI and sII hydrates by affecting the interaction with water. However, at t-$BuNH_2$ concentrations closer to sII stoichiometry (5.56 mol %), we measured 128 mL CH_4/g (∼6.86 wt %), at ∼0.083 MPa pressure and 297 K; the gas storage capacity remained the same even with the t-$BuNH_2$ concentration lowered to ∼1.0 mol % (see Figure 5). Note that NMR studies[8,10,22] indicated the cage occupancy of methane to be $\theta_s^{sII} = 0.7413$ and $\theta_l^{sII} = 0.4359$ for binary hydrates (t-$BuNH_2$ ∼1.0 mol %). Moreover, the cage occupancy was reported to be $\theta_s^{sII} = 0.7628$ and $\theta_l^{sII} = 0.1773$ in binary hydrates with lower t-$BuNH_2$ concentration (0.85 mol %).[8,10] The small cage occupancy was reported as $\theta_s^{sII} = 0.7875$ for binary hydrates with t-$BuNH_2$ concentration between 4.0 and 5.56 mol %, with t-$BuNH_2$ molecules occupying the large cages.[10] The methane storage capacity in these cases could be estimated to be 8.12, 6.93, and 6.23 wt %. We observed an average storage capacity of 6.86 wt % for 5.56 > t-$BuNH_2$ > 1.0 mol %, in close agreement with these results. On further decreasing the t-$BuNH_2$ concentration (<1.0 mol %), pure methane hydrate (sI) was formed, and the methane storage capacity was marginally increased to 190 mL CH_4/g (∼10.13 wt %), corroborating the NMR results, which reported dominance of the sI component in similar P,T conditions.[8,10,19]

Conclusions

The results shown here demonstrate that the structural transformation (sVI to sII) of t-$BuNH_2$ hydrate pressurized with methane was clearly observed from the PXRD patterns. Signatures of sII were more prominent (with no trace of sVI) for binary hydrates with 9.31 mol % > t-$BuNH_2$ > 5.56 mol %. The experiments indicate that sVI is unstable when pressurized with coguest molecules (methane or hydrogen) in binary hydrates. The Raman spectroscopic data suggested that the methane molecules occupy the small and vacant large cages of sII. The methane storage capacity in this system is nearly doubled in hydrates, with 5.56 mol % > t-$BuNH_2$ > 1.0 mol %, and the average is ∼6.86 wt % (∼128 mL/g). The Raman spectroscopic results also support earlier data on the dominance of sI in binary hydrates (t-$BuNH_2$ + CH_4) with lower t-$BuNH_2$ molar concentrations.

Acknowledgment. We acknowledge funding from NSF-REMRSEC [DMR 0820518]. P.S.R.P. is thankful to the Director, NGRI Hyderabad, for granting the sabbatical leave in the Center for Hydrate Research at the Colorado School of Mines. A.K.S. acknowledges the support from DuPont as a DuPont Young Professor.

Supporting Information Available: PXRD patterns of pure t-$BuNH_2$, CH_4 + t-$BuNH_2$, and H_2 + t-$BuNH_2$ hydrates synthesized using the t-$BuNH_2$ (5.56 mol %) clathrate hydrate as starting material. This material is available free of charge via the Internet at http://pubs.acs.org.

References and Notes

(1) Makogon, Y. F.; Holditch, S. A.; Makogon, T. Y. *J. Pet. Sci. Eng.* **2007**, *56*, 14–31.

(2) Sloan, E. D.; Koh, C. A. *Clathrate Hydrates of Natural Gases*, 3rd ed.; CRC Press, Taylor & Francis Group: Boca Raton, FL 2008.

(3) Khokhar, A. A.; Gudmundsson, J. S.; Sloan, E. D. *Fluid Phase Equilib.* **1998**, *150−151*, 383–392.

(4) McMullan, R. K.; Jeffrey, G. A.; Jordan, T. H. *J. Chem. Phys.* **1967**, *47*, 1229–1234.

(5) Jeffrey, G. A. In *Inclusion Compounds*; Atwood, J. L., Davies, J. E. D., MacNicol, D. D., Eds.; Academic Press: London, 1984; Vol. 1, pp 135−190.

(6) Udachin, K. A.; Ratcliffe, C. I.; Ripmeester, J. A. *Angew. Chem.* **2001**, *113*, 1343–1345.

(7) Strobel, T. A.; Koh, C. A.; Sloan, E. D. *Fluid Phase Equilib.* **2007**, *261*, 382–389.

(8) Kim, D. Y.; Lee, J.; Seo, Yu.-T.; Ripmeester, J. A.; Lee, H. *Angew. Chem.* **2005**, *117*, 7927–7930.

(9) Prasad, P. S. R.; Sugahara, T.; Sum, A. K.; Sloan, E. D.; Koh, C. A. *J. Phys. Chem. A* **2009**, *113*, 6540–6543.

(10) Kim, D. Y.; Park, Y.; Lee, J.; Ripmeester, J. A.; Lee, H. *J. Am. Chem. Soc.* **2006**, *128*, 15360–15361.

(11) The software programs Checkcell developed by Laugier, L.; Bochu, B., Laboratoire des Materiaux et du Genie Physique, Ecole Superieure de Physique de Grenoble, and PowderX developed by Cheng, D., Institute of Physics, Beijing, are available at http://www.ccp14.ac.uk.

(12) Staben, D.; Mootz, D. *J. Inclusion Phenom. Mol. Recognit. Chem.* **1995**, *22*, 145–154.

(13) Kipkemboi, P. K.; Easteal, A. J. *Can. J. Chem.* **2002**, *80*, 789–795.

(14) Prasad, P. S. R.; Prasad, K. S.; Thakur, N. K. *Spectrochim Acta, Part A* **2007**, *68*, 1096–1100.

(15) Prasad, P. S. R.; Sowjanya, Y.; Prasad, K. S. *Vibr. Spectrosc.* **2009**, *50*, 319–323.

(16) Schicks, J. M.; Naumann, R.; Erzinger, J.; Hester, K. C.; Koh, C. A.; Sloan, E. D. *J. Phys. Chem.* **2006**, *110*, 11468.

(17) Li, J.; Ross, D. K. *Nature* **1993**, *365*, 327–330.

(18) Park, Y.; Cha, M.; Shin, W.; Lee, H.; Ripmeester, J. A. *J. Phys. Chem. B* **2008**, *112*, 8443–8446.

(19) Yasuda, K.; Takeya, S.; Mami Sakashita, M.; Yamawaki, H.; Ohmura, R. *J. Phys. Chem. C* **2009**, *113*, 12598–12601.

(20) Susilo, R.; Alavi, S.; Ripmeester, J.; Englezos, P. *Fluid Phase Equilib.* **2008**, *263*, 6–17.

(21) Seo, Y.; Lee, J.; Kumar, R.; Moudrakovski, I. L.; Lee, H.; Ripmeester, J. *Chem. Asian J.* **2009**, *4*, 1266–1274.

(22) Kim, D. Y.; Park, Y.; Lee, H. *Catal. Today* **2007**, *120*, 257–261.

JP906492J